Understanding the Surface Properties and Rheology of Silica Suspension Mediated by Comb-type Poly (Acrylic Acid)/Poly (Ethylene Oxide) (PAA/PEO) Copolymer: Effect of Salinity

Dingzheng Yang[1,§], Bin Yan[2,§], Li Xiang[1], Haolan Xu[3], Xiaogang Wang[4,], Hongbo Zeng[1,*]*

[1]*Department of Chemical and Materials Engineering, University of Alberta, Edmonton, AB, T6G 1H9, Canada*

[2]*College of Light Industry, Textile & Food Engineering, Sichuan University, Chengdu, 610065, China*

[3]*Future Industries Institute, University of South Australia, SA 5095, Australia*

[4]*Colleage of Material Science & Engineering, Heavy Machinery Engineering Research Center of Education Ministry, Taiyuan University of Science and Technology, Taiyuan 030024, China*

[§]*D. Yang and B. Yan contributed equally to this work*

***Email:** hongbo.zeng@ualberta.ca, Phone: +1-780-492-1044 ; or Email : wxg@tyust.edu.cn*

Abstract

Understanding the surface properties and rheology of colloidal suspensions in the presence of polymer additives with high salinity is of great importance in formulating construction materials, and optimizing process conditions in mining and petroleum industry. In this work, the surface properties and rheology of model spherical silica aqueous suspension mediated by a comb-type poly(acrylic acid)/poly(ethylene oxide) (PAA/PEO) copolymer at various salt concentrations have been investigated. Adsorption measurements using Quartz Crystal Microbalance with Dissipation monitoring (QCM-D) align well with zeta potential tests, and show that polymer adsorption on silica surfaces is enhanced at higher salinity condition (i.e., 3 M NaCl) than the lower salinity case (i.e., 1 mM NaCl) due to the suppression of electrical double layer. Surface Forces Apparatus (SFA) measurements reveal that for interactions between two mica surfaces (the basal plane of which has similar structure as silica) at high polymer concentration (e.g., 2 wt %) steric repulsion dominates in 1 mM NaCl while bridging attraction is observed in 3 M NaCl. Surface force measurements agree with rheological results on silica suspensions with 0.5 to 2 wt % of PAA/PEO addition, which shows significant decrease on yield stress in 1 mM NaCl due to steric repulsion but insignificant variation on yield stress in 3 M NaCl due to attractive bridging interactions. This work provides useful information regarding the surface properties and rheological properties of comb-type polymer mediated silica suspensions under different salinity, with implications on designing and processing complex colloidal suspensions with polymer additives for various applications.

1. Introduction

Colloidal suspensions in aqueous media of different salinity conditions are encountered in various industrial products and processes, such as construction materials,[1] tailings management,[2-4] drilling mud,[5] and enhanced oil recovery.[6] Understanding the flow behavior and rheological properties of such colloidal suspensions, and how the rheology can be manipulated by tuning water chemistry, especially using polyelectrolytes, are of great importance in optimizing the formulations and processing conditions in industrial applications.[7-10] Comb-type copolymers with an adsorbing backbone and nonadsorbing side chains are particularly interesting due to their good dispersion performance in water of high salinity.[11-12] Comb-type polymer dispersants have been reported to be effective for colloidal systems including cemented carbide,[13] kaolinite,[14] magnesia,[15] and silica.[16]

Flatt et al. studied the effect of comb-type methacrylic acid/alkyleneglycol methacrylate copolymer on surface forces between calcium silica hydrate using AFM, and observed a monotonic steric hindrance between two solid surfaces with full polymer coverage at basic conditions.[11] Neuville et al. suggested that at basic conditions electrical double layer repulsion generated from negatively charged comb-type methacrylic acid/ethylene oxide copolymer was important for dispersing concentrated gypsum slurries.[7] For the above colloidal systems with polymer additives reported previously, steric repulsion was commonly observed at high pH where negatively charged polymer chains tended to extend. Hommer measured the streaming potential of comb-type acrylic acid/ethylene oxide copolymer and found a near zero charge density at pH 2-3 due to the protonation of acrylic acid backbone.[17] Under such low pH conditions, the polymer chains tended to collapse into a compact structure and provided poorer dispersing effect.[14] All the above studies focused on colloids with polymers in pure water or

aqueous suspensions of low salinity. No report is available on colloidal suspensions with comb-type polymeric dispersant under high salinity condition.

The rheological behavior of colloidal suspensions, such as yielding, is largely dependent on the microstructure (i.e., arrangement of particles in the suspension, such as mean inter-particle distance),[18-19] volume fraction,[20] particle size and size distribution, as well as colloidal forces.[21-24] Given the volume fraction and geometry of the particles in the suspension, the colloidal forces, microstructure and resulting rheology could be tuned by varying the water chemistry (i.e., pH, salt and chemical additives like polymers). Savarmand and Carreau interpreted the behavior of yield stress and shear viscosity of spherical silica colloids in low salinity solutions in terms of surfaces forces base on the Derjaguin-Landau-Verwey-Overbeek (DLVO) model.[25] At high salt concentration (e.g., more than 0.5 M of monovalent electrolyte), non-DLVO forces became important and governed the microstructural and rheological properties of concentrated colloidal spheres.[26] Franks revealed a pronounced increase in shear yield stress of silica suspensions at high pH with high concentration of monovalent salt, which had been presumably attributed to an attractive ion-correlation force.[10] The inter-particle distance had also been considered as a critical factor that caused significant increase on the yield stress of alumina suspension by Franks and Boger.[26] Whitby et al. investigated the effect of poly (acrylic acid)/poly (ethylene oxide) comb-type copolymer on surface forces and rheology of colloidal silica suspension at low salinity.[16] The rheology of colloidal suspensions mediated by comb-like copolymers in high saline water is still not clear yet.

In this work, we have used spherical silica particles and a comb-type PAA/PEO copolymer as a model system and attempted to correlate the surface forces between colloidal particles in the presence of polymers and their bulk rheological properties. Polymer adsorption and zeta

potential measurements were also conducted under different pH and salinity conditions to better understand the surface forces and rheology results. Our study covered a broad range of salt concentration from 1 mM to 3 M. Three salt concentrations (1 mM, 0.5 M and 3 M) were selected to represent different scenarios from the DLVO force controlled system to non-DLVO force controlled system. This work provides useful results regarding the effects of solution salinity on the surface properties and rheology behaviors of colloidal suspensions with polymer additives, with implications on polymer-mediated colloids in a wide range of industrial applications.

2. Materials and Methods

2.1 Materials

Silica particles were purchased from Alfa Aesar (Ward Hill, MA). Particle size distribution was determined by light scattering using a Zeta Nanosizer (Malvern, UK) by dispersing 0.1 g silica particles in 100 ml Milli-Q water, as shown in Figure 1(a). Mean particle size was about 548.5 nm. Morphological analysis on silica particles was carried out using JAMP-9500F Scanning Electron Microscope (SEM) at the Alberta Center for Surface Engineering and Science (University of Alberta). As shown in Figure 1(b), spherical shape of silica particle is observed, the particle size is comparable to the mean size obtained from light scattering method using Zeta Nanosizer.

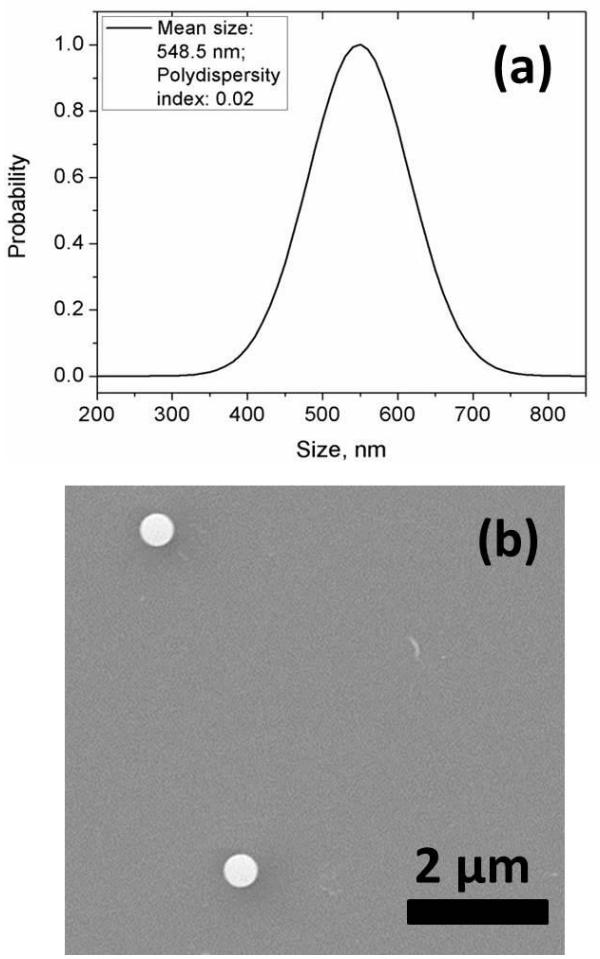


Figure 1. Particle size distribution (a) and morphology (b) of silica in 1 mM NaCl determined by light scattering using a Zeta Nanosizer and SEM, respectively.

Poly (acrylic acid)/poly (ethylene oxide) comb-type copolymer (Melflux 1641F, BASF) had molecular weight in a range of 20,000 Da. Sodium chloride (NaCl, ACS analytical grade, Sigma-Aldrich) was used for preparing the salt solutions for both surface force measurements and rheological measurements. Analytical grade hydrochloric acid (HCl) and sodium hydroxide (NaOH, Sigma-Aldrich) were used to adjust solution pH values. Milli-Q water with a resistivity of 18.2 $M\Omega cm^{-1}$ was used for preparing all the aqueous solutions in this work.

2.2 Zeta Potential Measurements

0.1 g silica powder was dispersed in 100 ml Milli-Q water of various NaCl concentrations (0.001 to 0.5 M), and the pH of the aqueous suspensions was then adjusted to a desired value. The prepared silica suspension was dispersed using an ultrasonic bath (Fisher Scientific) for 10 minutes before zeta potential measurements. The zeta potential of the silica suspensions was determined using a Zeta Nanosizer ZSP (Malvern, UK).

2.3 Quartz Crystal Microbalance with Dissipation Monitoring (QCM-D)

Polymer adsorption was monitored with a QCM-D (Q-Sense E1, Gothenborg, Sweden) at a controlled temperature of 20.0±0.1°C. The quartz crystal oscillators or sensors used were thin AT-cut quartz crystals with a diameter of 14 mm and fundamental shear oscillation frequency of 5 M Hz. The sensors were coated with a thin film of silicon dioxide with a thickness of 50 nm. The variations of frequency (Δf) and dissipation (ΔD) of the crystals upon imposing AC signals were monitored simultaneously at following resonance frequencies: 5, 15, 25, 35, 45, 55 and 75 MHz. The third and fifth overtones were used to calculate the adsorbed mass. While the Sauerbrey model[27] is suitable for the case of adsorbing thin and rigid layers, Voigt viscoelastic model embedded in the Q-Sensor software was more suitable for adsorption of soft and thick polymer layers on the sensors. As a rule of thumb, the Sauerbrey model is suitable if $\Delta D/\Delta f << 4\times10^{-6}$.[28] In this work, considering large $\Delta D/\Delta f$ ratio measured, the Voigt viscoelastic model would be used to determine the adsorbed mass of the polymers. The general procedure for the QCM-D tests involved sequentially flowing the following fluids through the QCM-D chamber: (1) NaCl solution of selected salt concentration and pH condition (as background solution); (2) polymer solution with desired concentration at the same salt concentration and pH conditions; (3) background solution. A flow rate of 0.15 ml/min was used for all the experiments.

2.4 Surface Forces Apparatus (SFA) Measurements

A surface forces apparatus was used to measure the surface forces between two molecular smooth mica surfaces (the basal plane of which has similar structure as silica) at various solution pH, salt concentrations and polymer concentrations. The detailed experimental setup of SFA experiments have been reported previously.[14, 29-35] Briefly, back-silvered (~50 nm silver) thin mica sheets (1-5 μm) were glued onto two cylindrical silica discs (radius~2 cm). The two surfaces were mounted into the SFA chamber in a crossed-cylinder configuration, the interactions of which were locally equivalent to the interaction between a sphere of the same radius and a plane according to the Derjaguin approximation. A desired polymer solution was then injected between the two mica surfaces. Force measurements were conducted after the system was equilibrated for 1.5 h. During a typical normal force measurement, the two surfaces were brought to approach each other till a so-called hard-wall separation was reached (which barely changed with increasing the normal load or pressure). The two surfaces were kept in contact under the maximum load for ~1 min before they were separated. The surface separation and deformation were monitored in situ and in real time through the multiple beam interferometry technique by using the optical interference fringes of equal chromatic order (FECO). The surface forces were determined based on the Hooke's Law.

2.5 Rheology Tests

A TA AR-G2 stress-controlled rheometer (TA Instruments, DE) equipped with a Peltier temperature control system was employed for the rheological studies. The concentric cylinder geometry was chosen to minimize the effect of sedimentation of particles. The surfaces of the concentric cylinder sample holder were sand blasted in order to prevent the wall slip. The

volume fraction of silica used was 0.3, i.e., 52.3 wt%. The prepared silica suspensions with desired water chemistry were homogenized using a mechanical mixer, followed by ultrasonication using a Sonic Dismembrator (Model 500, Fisher) at 30% of the total power for 2 minutes.[24]

The stress growth, or stress overshoot method, was used to obtain the shear yield stress by controlling the strain rate.[36] A shear strain rate of 0.005 s^{-1} was used for the tests, because hydrodynamic and thixotropic effects were not observed at such shear strain rate. All the samples were pre-sheared for 60 s at 1000 s^{-1} followed by 120 s rest. The temperature used in this study was 20 ±0.5 °C.

3. Results and Discussion

3.1 Zeta Potential

The zeta potential values of silica particles under various salt concentrations and pH conditions have been measured by a zeta Nanosizer and are shown in Figure 2. It is noted that due to limitations of the instrument for measurements under very high salinity condition, the zeta potential of silica suspension in 0.5 M NaCl is measured rather than in 3 M NaCl solutions to understand the effect of high salt concentration. Silica exhibits a isoelectric point (IEP) of 2 above which increasingly negative zeta potential is observed as also reported previously, which is correlated to the increasing deprotonation of silanol groups with a structural transformation from SiOH to SiO^-.[10] The absolute value of zeta potential is found to decrease with increasing the salt concentration.

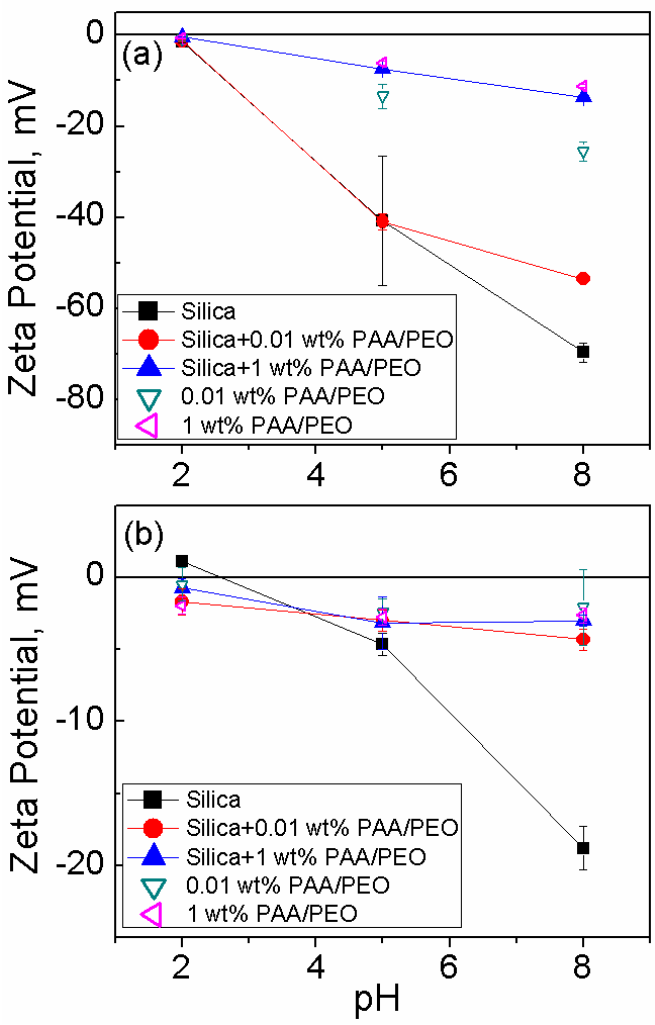


Figure 2. Zeta potential of silica suspensions with and without PAA/PEO copolymer of different concentrations at various solution pH conditions in (a) 1 mM NaCl, and (b) 0.5 M NaCl.

Zeta potential of PAA/PEO at various pH and salt concentrations was also determined, as shown in Figure 2. It is found that the acid dissociation constant of PAA/PEO comb-like polymer is about 2. With increasing pH, PAA/PEO becomes more negatively charged, due to the deprotonation of carboxylic groups on the polymer backbone. In Figure 2(a), it is found that zeta potential of PAA/PEO copolymer decreases with the increase of polymer concentration from

0.01 to 1 wt%. Under high salinity condition as shown in Figure 2(b), the absolute value of the zeta potential of PAA/PEO decreases due to the compression of electrical double layer.

As shown in Figure 2, zeta potential of silica becomes less negative after adding 0.01 wt% PAA/PEO copolymer, and the magnitude of zeta potential decreases further upon increasing the polymer concentration to 1 wt%. Zeta potential of silica associated with polymer in 0.5 M NaCl solution is found lower than that in 1 mM NaCl solution, which is caused by compression of electrical double layer.

3.2 QCM-D adsorption tests

The adsorption measurements of PAA/PEO copolymer on silica sensor were conducted by using a QCM-D. Variations on frequency and dissipation of the silica sensor due to the adsorption of polymers in 1 mM NaCl solution are shown in Figure 3. In Figure 3(a), 1 mM NaCl solution (pH 2) is firstly injected into the system as a background solution to establish the baseline for monitoring the frequency change. The addition of 0.01 wt% polymer solutions leads to a shift on the frequency and dissipation. Both silica surface and carboxylic groups on the polymer backbone are highly protonated at pH 2 as indicated in Figure 2. The hydrogen bonding interaction between the polymer chains and silica surface plays a dominating role in the polymer adsorption. Successively introducing the 1 mM NaCl solution (pH 2) does not cause any obvious change of the frequency, indicating that adsorbed polymers could not be removed by the background saline solution.

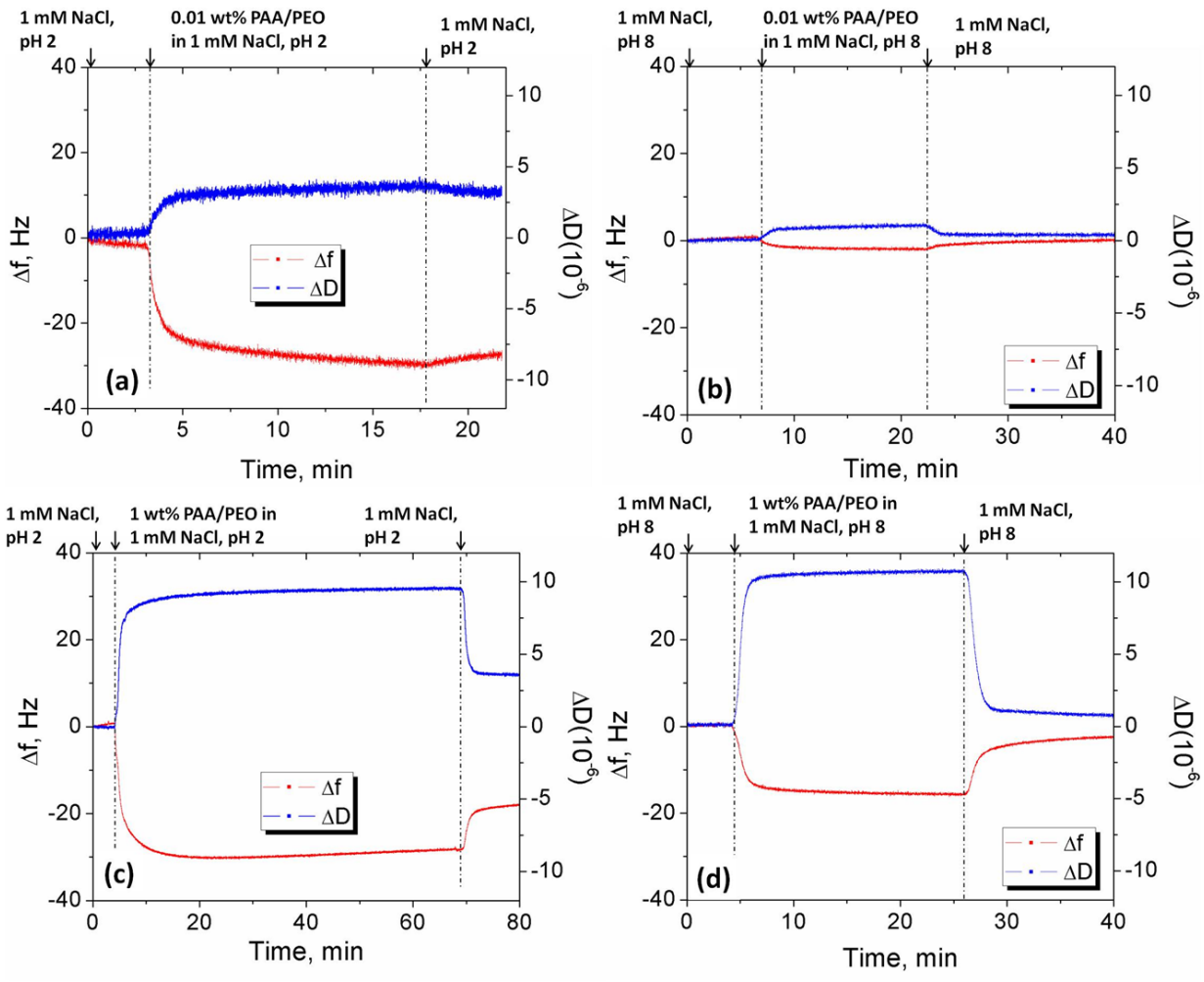


Figure 3. Changes of frequency *Δf* and dissipation *ΔD* associated with the adsorption of PAA/PEO in 1 mM NaCl solution at various pH conditions on QCM-D silica sensors: (a) 0.01 wt% PAA/PEO at pH 2, (b) 0.01 wt% PAA/PEO at pH 8, (c) 1 wt% PAA/PEO at pH 2, (d) 1 wt% PAA/PEO at pH 8.

As shown in Figure 3(b), fixing the NaCl concentration 1 mM and polymer concentration 0.01 wt% while increasing the solution pH from 2 to 8, it is found that the polymer adsorption has been significantly weakened indicated by frequency shift of about 5 % of that at pH 2. At pH 8,

both silica surface and the carboxylic groups on the PAA/PEO comb-like polymer are highly deprotonated and negatively charged as indicated in Figure 2. The long-range electrostatic repulsion between the PAA/PEO chains and silica could inhibit the adsorption of polymers. As shown in Figure 3(c) and (d), with the PAA/PEO concentration increasing to 1 wt%, the frequency shift increases at both pH 2 and 8, indicating enhanced polymer adsorption. The mechanism of adsorption of PAA/PEO onto silica in 1 mM NaCl solutions under various pH conditions is proposed and illustrated in Figure 5(a).

Variations on frequency and dissipation of the silica sensor due to the adsorption of polymers in 3 M NaCl solution are shown in Figure 4. It is found that the high salinity condition (3 M NaCl) at pH 8 significantly enhances the polymer adsorption on silica as compared to the low salinity case (1 mM NaCl in Figure 3). Under high salinity condition, the Debye length of the electrical double layer has been compressed to be less than 1 nm, and the electrostatic repulsion between PAA/PEO and silica has been drastically supressed.

The effect of polymer concentration has been also investigated. As shown in Figure 4(c) and (d), larger frequency shift and enhanced polymer adsorption are detected with increasing the PAA/PEO concentration from 0.01 wt% to 1 wt% while keeping the pH and NaCl concentration the same. It is also found that while the adsorbed polymers are more stable during rinsing by background NaCl solution at pH 2, the adsorbed polymers could be easily removed by rinsing of the background NaCl solution at pH 8. The mechanism of adsorption of PAA/PEO onto silica in 3 M NaCl solution under various pH conditions is proposed and illustrated in Figure 5(b).

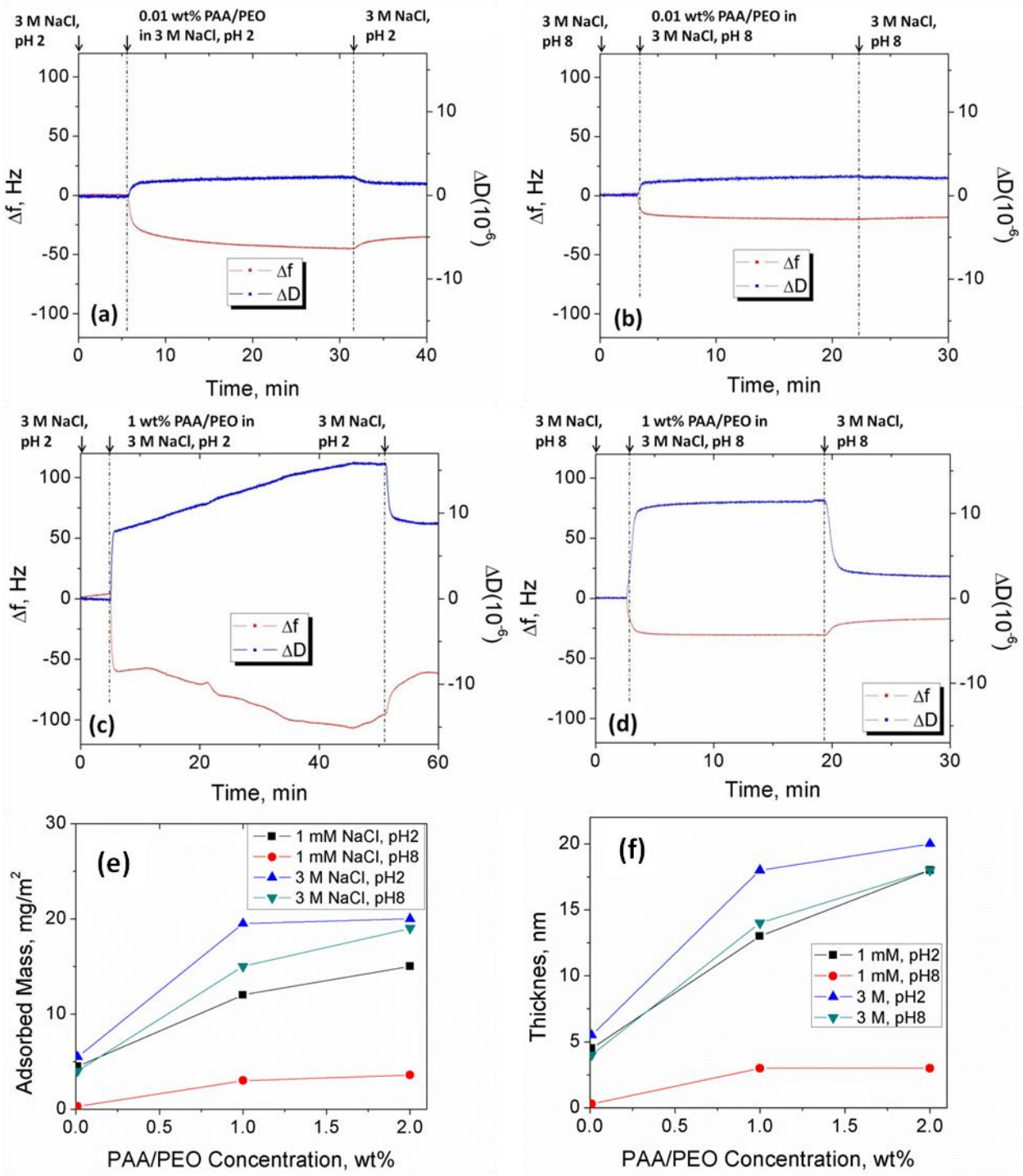
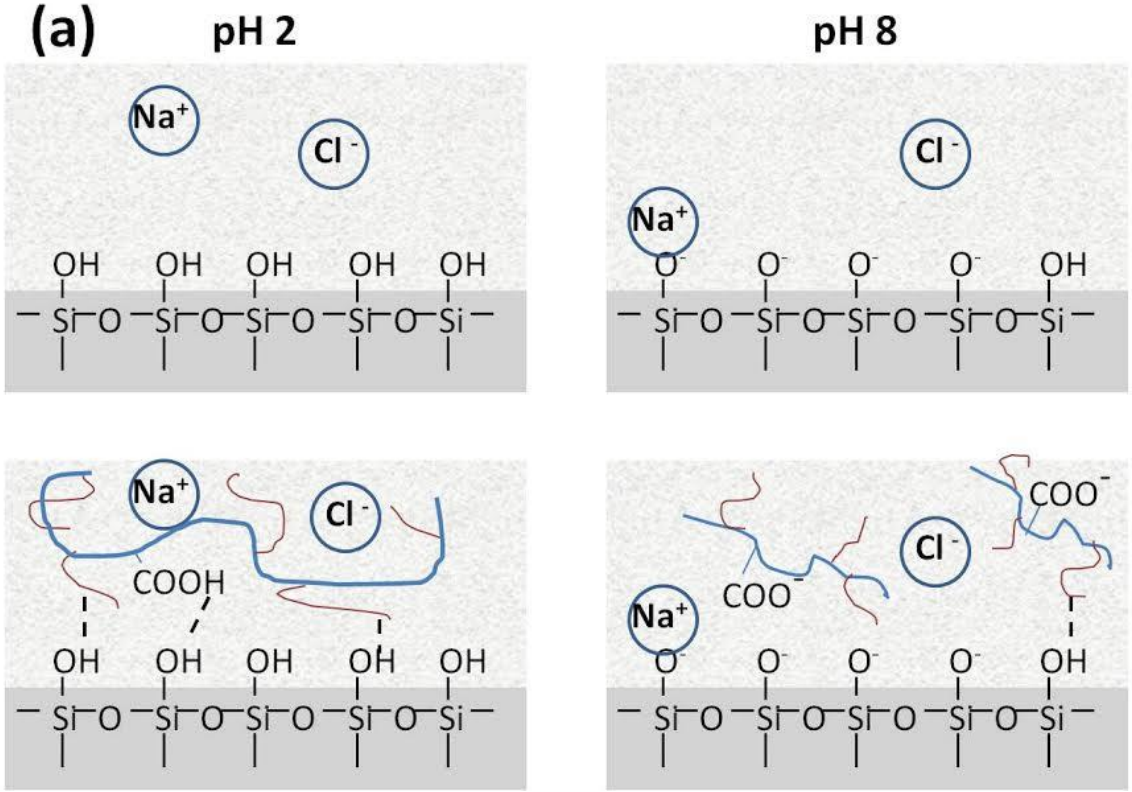


Figure 4. Changes of frequency *Δf* and dissipation *ΔD* associated with the adsorption of PAA/PEO in 3 M NaCl solution at various pH on QCM-D silica sensors: (a) 0.01 wt% PAA/PEO at pH 2, (b) 0.01 wt% PAA/PEO at pH 8, (c) 1 wt% PAA/PEO at pH 2, (d) 1 wt%

PAA/PEO at pH 8; (e) summary on adsorbed mass of PAA/PEO onto silica sensor at various pH and salt concentrations determined by QCM-D; (f) thickness of PAA/PEO layer adsorbed onto silica sensor at various pH and salt concentrations.

The QCM-D adsorption curves shown in Figures 3 and 4 were analyzed using the Voigt viscoelastic models to quantify the mass and thickness of the adsorbed PAA/PEO polymer.[37] Figure 4 (e) and (f) show the adsorbed mass and thickness as a function of bulk polymer concentration at various salt concentration and pH conditions, respectively. It is observed that with increasing the bulk polymer concentration, the adsorbed mass and thickness increase more significantly at a polymer concentration below 1 wt% than that at relatively high polymer concentration (e.g., 2 wt%).



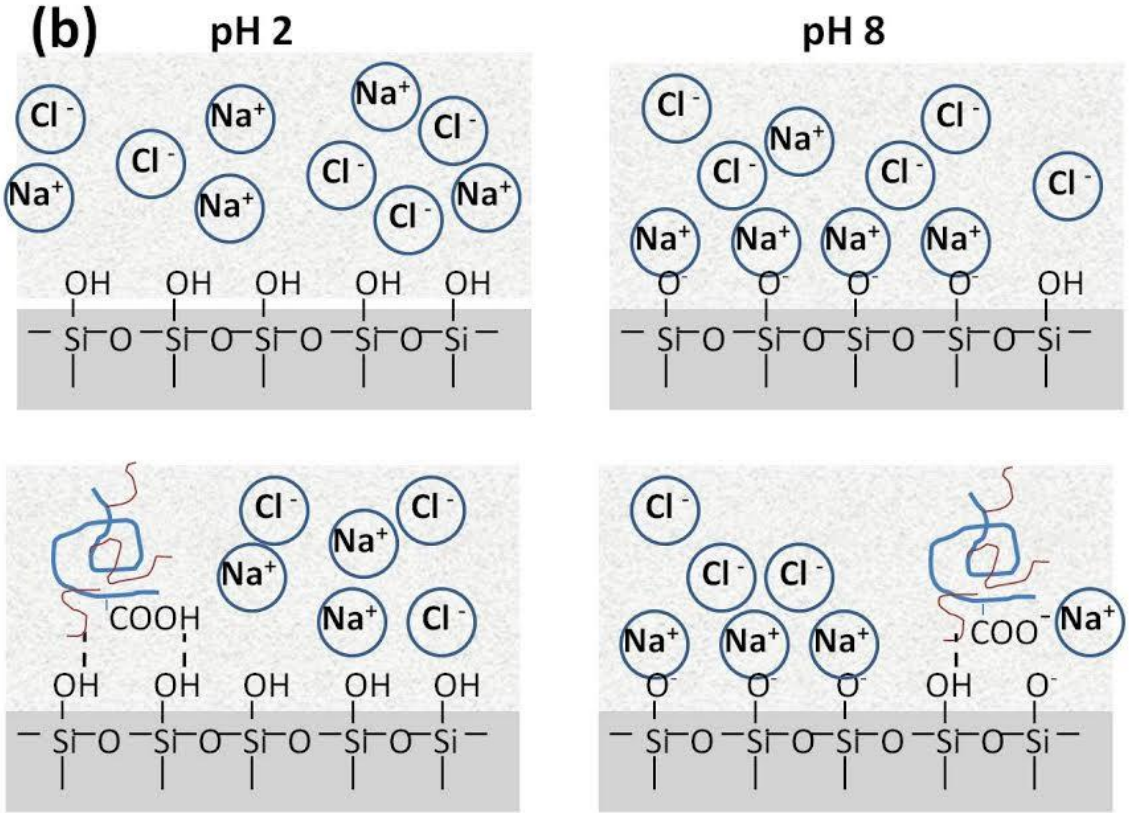


Figure 5. Schematic for the adsorption mechanism of PAA/PEO copolymer in saline solutions at pH 2 and pH 8 with (a) 1 mM NaCl, and (b) 3 M NaCl.

3.3 Surface force measurements

To probe the interactions between silica spheres, surface force measurements were carried out between two model silica surfaces (i.e., mica, the basal plan of which has similar surface composition as silica) in the presence of PAA/PEO polymer. Figure 6 shows force-distance curves during approaching and separation of two mica surfaces in PAA/PEO copolymer solutions containing 1 mM NaCl. As shown in Figure 6(a) and (c) in 0.1 wt% polymer solutions, adhesion F_{ad}/R of 4.9 and 3.2 mN/m are measured through the separation force-distance curves

at pH 2 and pH 8, respectively. The adhesion is mainly caused by bridging effect of the adsorbed PAA/PEO chains confined between two mica surfaces. The bridging effect at pH 2 is stronger than that at pH 8 indicated by higher adhesion at pH 2. As shown in Figure 6(b) and (d), by increasing PAA/PEO concentration to 1.5 wt%, the adhesion F_{ad}/R during the separation of mica surfaces disappears. Repulsion is detected during approaching process of two mica surfaces at ~12 nm in 0.1 wt% PAA/PEO, and the repulsion range increases to 35 nm for the case of 1.5 wt% PAA/PEO at pH 2. At pH 8, the repulsion measured during approaching force curve starts at 20 nm in 0.1 wt% PAA/PEO, and slightly increases to 25 nm in 1.5 wt% PAA/PEO. The repulsion range during the approach process at pH 2 (Figure 6a and 6b) is found to be roughly double of the thickness of polymer adsorbed on silica sensor estimated from QCM-D measurements (which are about 5 and 16 nm for one polymer layer on the silica sensor in 0.1 wt% and 1.5 wt% of polymer, respectively), indicating that steric force between the PAA/PEO adsorbed on mica surfaces is the major contribution for the repulsive forces measured. At pH 8, both electrical double layer forces and the steric interactions of the adsorbed polymers contribute to the repulsion measured during approaching of the two surfaces in 1 mM NaCl (Figure 6c and 6d).

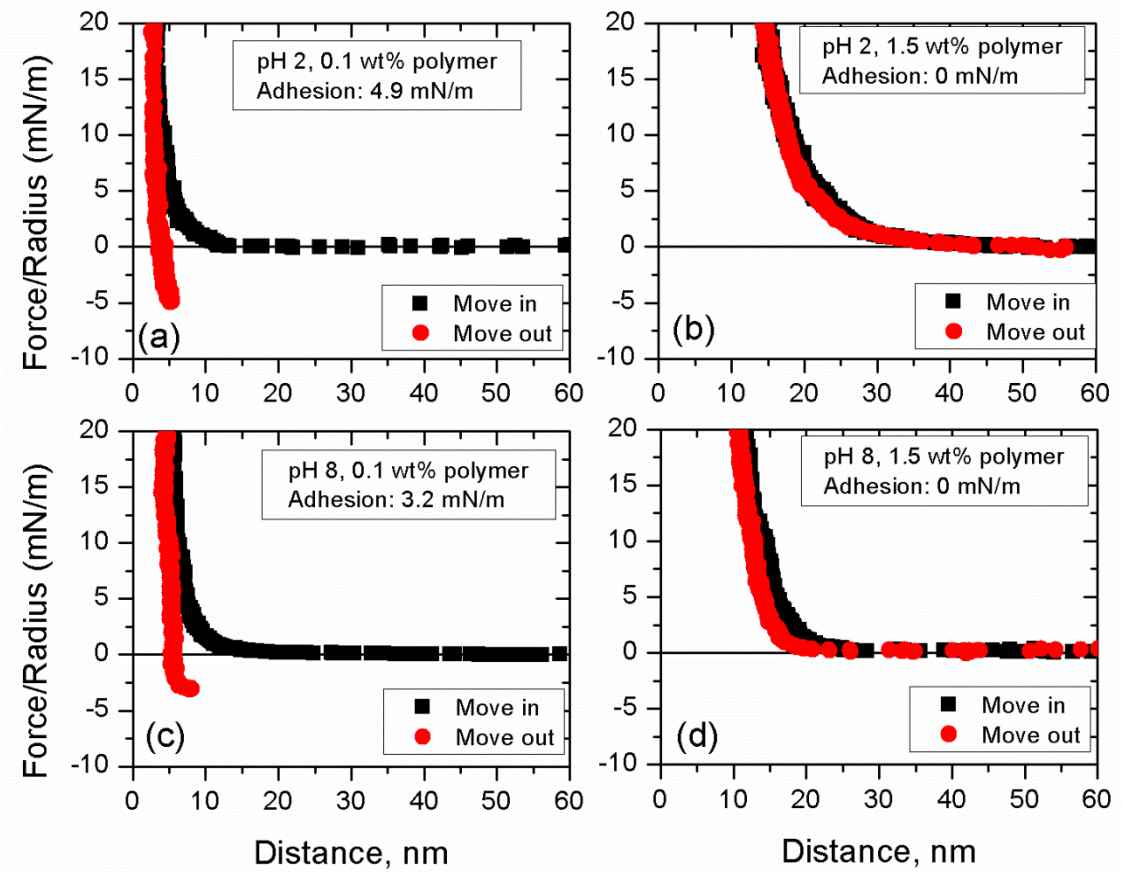


Figure 6. Force-distance profiles measured during approaching (moving in) and separation (moving out) of two mica surfaces in 1 mM NaCl solutions with (a) 0.1 wt% PAA/PEO at pH 2, (b) 1.5 wt% PAA/PEO at pH 8, (c) 0.1 wt% PAA/PEO at pH 2, and (d) 1.5 wt% PAA/PEO at pH 8.

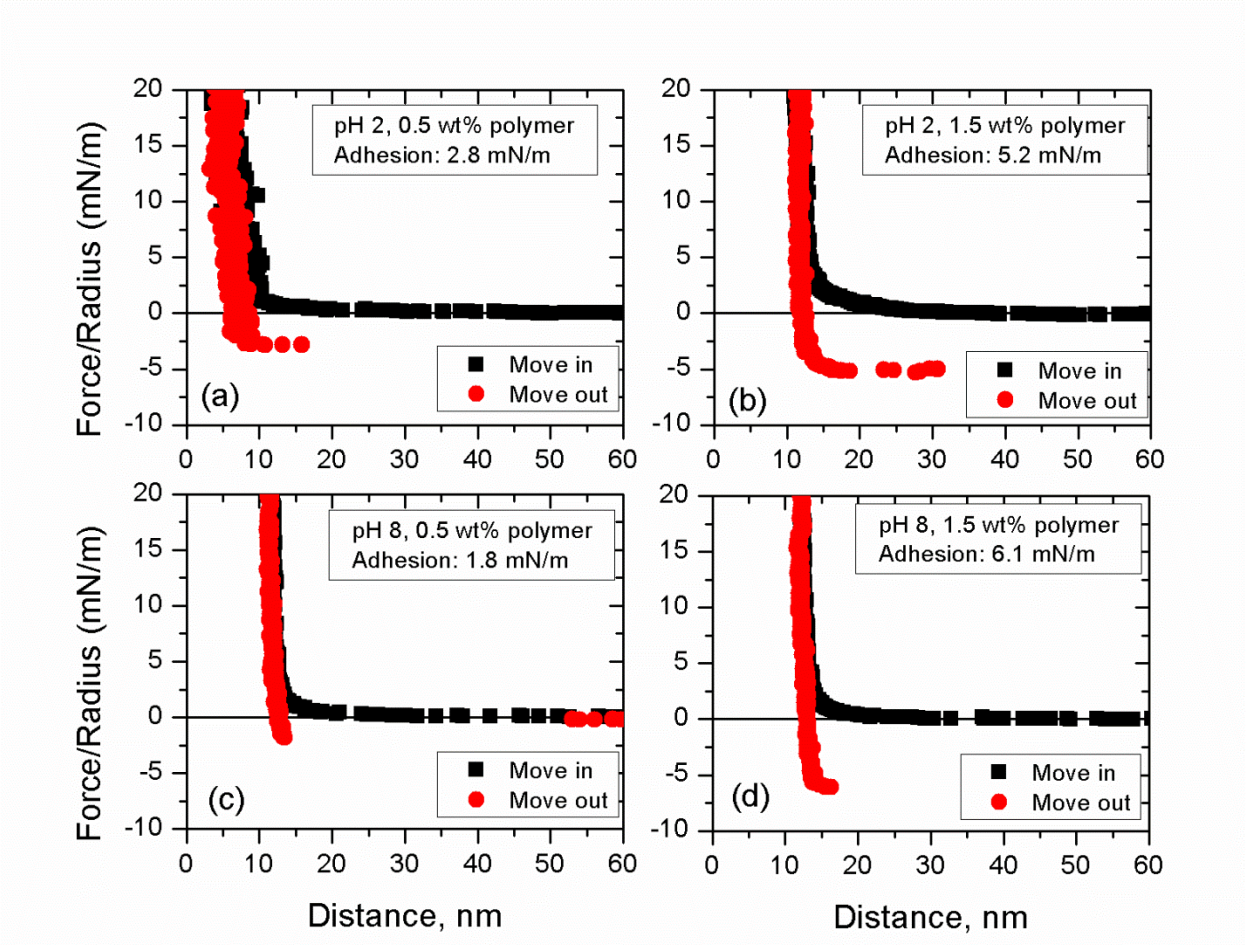


Figure 7. Force-distance profiles between two mica surfaces in 3 M NaCl solutions with (a) 0.5 wt% PAA/PEO at pH 2, (b) 1.5 wt% PAA/PEO at pH 8, (c) 0.5 wt% PAA/PEO at pH 2, (d) 1.5 wt% PAA/PEO at pH 8.

As shown as Figure 7, in 3 M NaCl solutions with 0.5 wt% PAA/PEO copolymer, adhesion F_{ad}/R of 2.8 and 1.8 mN/m are measured through the separation force-distance curves at pH 2 and pH 8, respectively. By increasing PAA/PEO concentration to 1.5 wt%, increased adhesions of 5.2 and 6.1 mN/m are detected at pH 2 and pH 8, respectively. In 3 M NaCl solutions, the charges from both mica and PAA/PEO copolymer tend to be significantly suppressed as shown in zeta potential measurements. The adhesion is mainly caused by bridging effect of the adsorbed

PAA/PEO chains between mica surfaces, contributed by H-bonding and van der Waals interactions as well as interpenetration of the confined PAA/PEO chains. Repulsion is detected during the approaching process which starts at ~20 and ~35 nm in 0.5 wt% and 1.5 wt% PAA/PEO at pH 2, respectively, at ~20 and ~25 nm in 0.5 wt% and 1.5 wt% PAA/PEO at pH 8, respectively. The above range of repulsion is found to be roughly double the thickness of polymer layer adsorbed on silica sensor detected in QCM-D measurements, which are about 11 and 17 nm at pH 2, 9 and 15 nm at pH 8 for one polymer layer adsorbed on the silica sensor in 0.1 wt% and 1.5 wt% polymer solutions, respectively. The above results indicate that steric interactions of the adsorbed polymer chains dominate the forces during the approaching of two mica surfaces under high salinity condition.

3.4 Rheology Tests

3.4.1 Silica suspension

The rheology of 30 vol% silica particles suspended in NaCl solutions with various salt concentrations and pH conditions is shown in Figure 8. In Figure 8(a), typical shear stress-strain profiles are shown to demonstrate the determination on the shear yield stress (i.e., stress growth or overshooting method).[36] At the initial stage of shearing, the shear stress grows roughly linearly with the strain due to the elastic deformation of the fluid. Once the shear deformation or strain exceed a critical value, i.e., yield strain, the fluid begins to yield. The local maximum shear stress corresponding to the yield strain is defined as the shear yield stress. It is found that the yield strain ranges from 0.01 to 1 % and increases with the yield stress. Exceeding the yield stress, the shear stress decreases and eventually reaches a steady state as indicated by a plateau of shear stress. The stress growth curve for the silica suspension in 1 mM NaCl solutions at pH 8

shows some noise at a strain larger than 0.1 %, which is mainly because the torque measured is very low (e.g., 0.04 $\mu N \cdot m$ at a strain of 1 %) and the value is close to the lower detectable limit of the stress controlled AR-G2 rheometer, i.e., 0.03 $\mu N \cdot m$.

The shear yield stress of silica suspension under various pH and NaCl concentrations is shown in Figure 8(b). In 1 mM NaCl solution, the yield stress is found to increase with the decrease of pH and it reaches a maximum at pH 2 where IEP of silica is observed (Figure 2a). The maximum yield stress at IEP is mainly caused by van der Waals attractive force among dispersed particles. An increased yield stress with decreasing pH from 8 to 2 is observed for silica in 0.5 M NaCl solutions, while an opposite trend of pH dependent yield stress for silica suspension is observed in 3 M NaCl solution. This is possibly because non-DLVO forces play a more important role than the DLVO interactions under high salinity condition. In 3 M NaCl solutions, the yield stress of silica suspension at the same pH increases significantly as compared to that in 1 mM and 0.5 M NaCl solutions. The significant increment of yield stress in high salt concentration conditions is possibly due to the following two reasons. Firstly, the magnitude of van der Waals force between particles increases. Under higher salt concentration conditions, the Hamaker constant slightly decreases due to the decrease of dielectric constant and increase of refractive index of the medium solution.[38-39] For example, Hamaker constant is 4.14×10^{-21} J between silica spheres in 3 M NaCl solutions, while it is 6.28×10^{-21} J in 1 mM NaCl solutions. On the other hand, the closest proximity between silica surfaces could decrease, caused by the increase of osmotic pressure between silica in higher salt solutions. As a result, van der Waals force could significantly increase, leading to a dramatic increase on yield stress. Secondly, in addition to the van der Waals force, additional attractive interactions between two surfaces, such as ion correlation force, could play a role.[40-41] The two silica surfaces adsorbed with counter-ions could

attract each other through mediated chloride ions or dipole interaction.[17] In addition, hydration force is considered to increase with the increase of salt concentration. Therefore, the observed attractions between silica at higher salt concentration are the results from competitions of the above mentioned DLVO and non-DLVO forces.

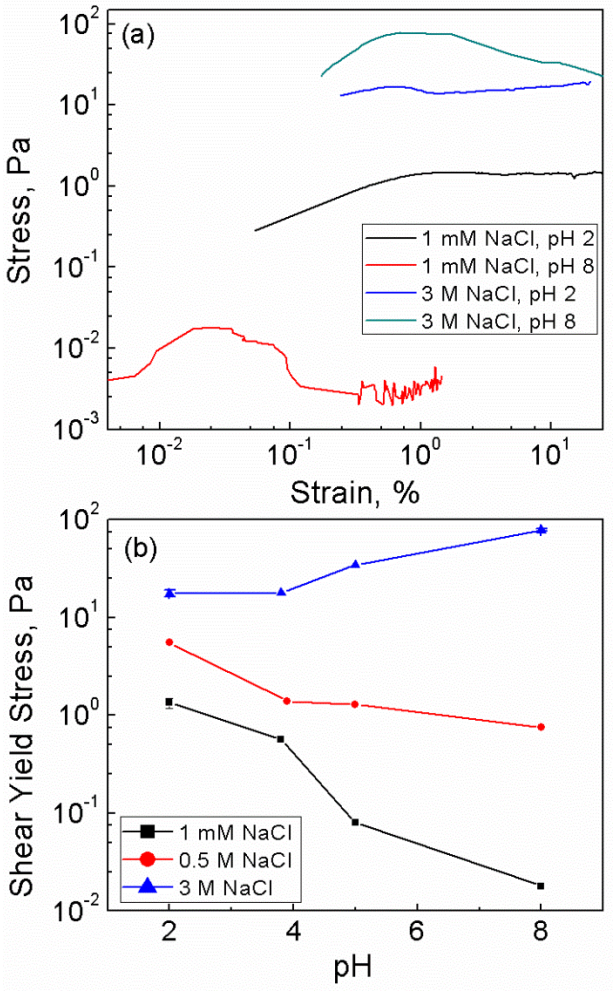


Figure 8. Shear yield stress of 30 vol% of silica particles in NaCl solutions with various salt concentrations and pH values. (a) Stress-strain profiles for yield stress determination; (b) Shear yield stress versus pH.

3.4.2 Silica in PAA/PEO copolymer solution

Rheological measurements on silica suspensions mediated by 0.01-2 wt% of PAA/PEO copolymers under various pH and salt concentrations are shown in Figure 9. Shear stress variation versus time at 0.005 s^{-1} of shear rate is shown in Figure 9(a), and the determined shear yield stress from these stress growth curves are summarized in Figure 9(b). It is found that the shear yield stress of silica suspension increases at PAA/PEO concentration from 0 to 0.5 wt%. Such increment on yield stress is mainly caused by bridging effect of PAA/PEO chains between silica particles, as demonstrated by QCM-D adsorption results and SFA force measurements. A schematic drawing on proposed mechanism of interaction between PAA/PEO mediated silica in NaCl solution at various pH is shown in Figure 10. As shown in Figure 9(b), the shear yield stress of silica suspension decreases at PAA/PEO concentration from 0.5 to 2 wt%, which is mainly caused by steric repulsion among the silica particles.

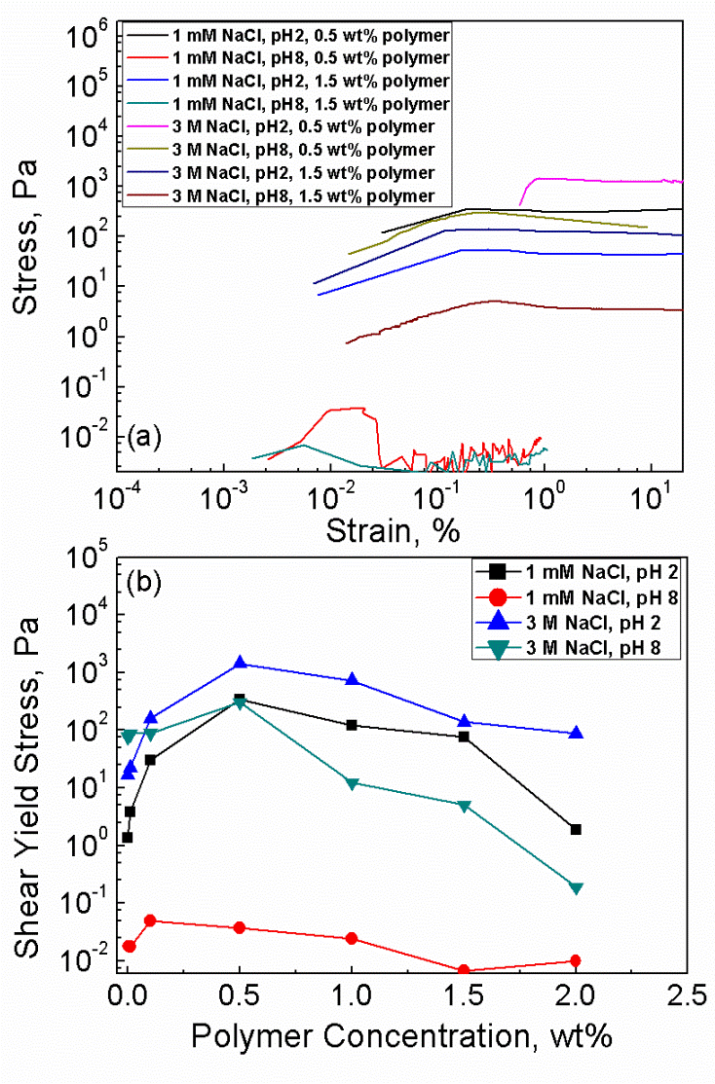
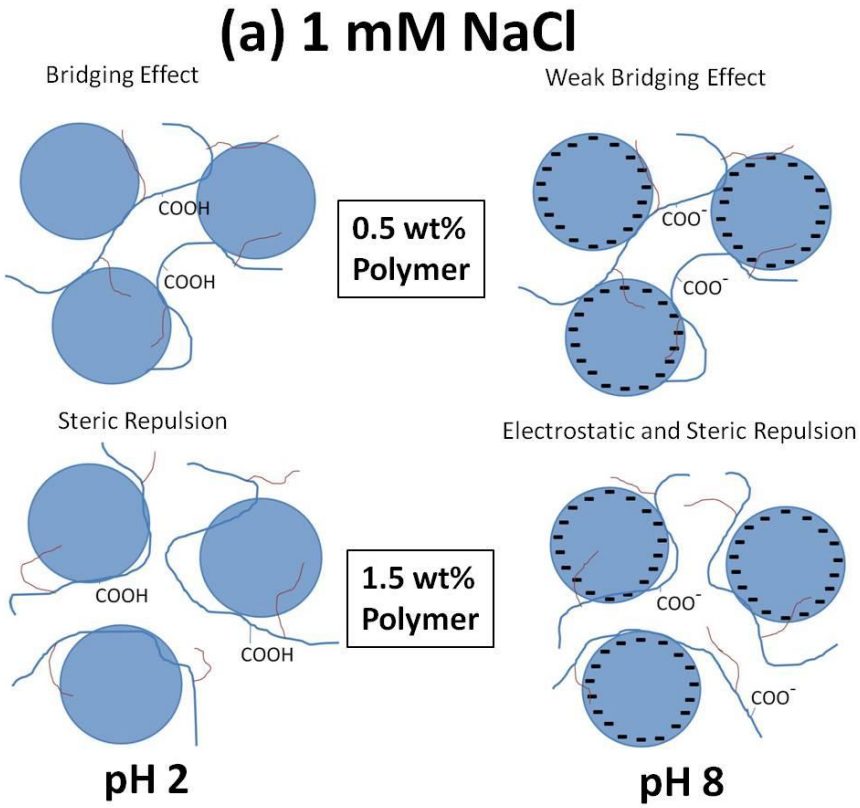


Figure 9. Shear yield stress of 30 vol% of silica particles associated with PAA/PEO copolymer in NaCl solutions with various salt concentrations and pH values. (a) Stress-strain profiles for yield stress determination; (b) Shear yield stress versus PAA/PEO concentration.

In 1 mM NaCl solutions, it is observed that the yield stress at pH 2 is 3-4 orders of magnitude higher than that at pH 8 at all PAA/PEO concentration. The much lower yield stress at pH 8 is mainly because of the electrostatic repulsions between silica particles, as proposed in Figure

10(a). In 3 M NaCl solutions, it is found that the yield stress at pH 2 is several times higher than that at pH 8 at PAA/PEO concentration above 0.5 wt%. Since the charges on both silica surface and polymer are significantly screened under high salinity condition, the decreased yield stress with increase of PAA/PEO concentration is mainly caused by the steric force rather than electrostatic repulsion, as proposed in Figure 10(b). It is interesting to find that at pH 2 in 3 M NaCl solutions the yield stress of silica suspension with addition of 2 wt% of PAA/PEO copolymer is still higher than that without any polymer addition. It is clearly shown that attraction is present between PAA/PEO mediated silica particles, which is most likely caused by H-Bonding attractions bridged by the polymer chains. Such phenomenon is well aligned to the SFA measurements.



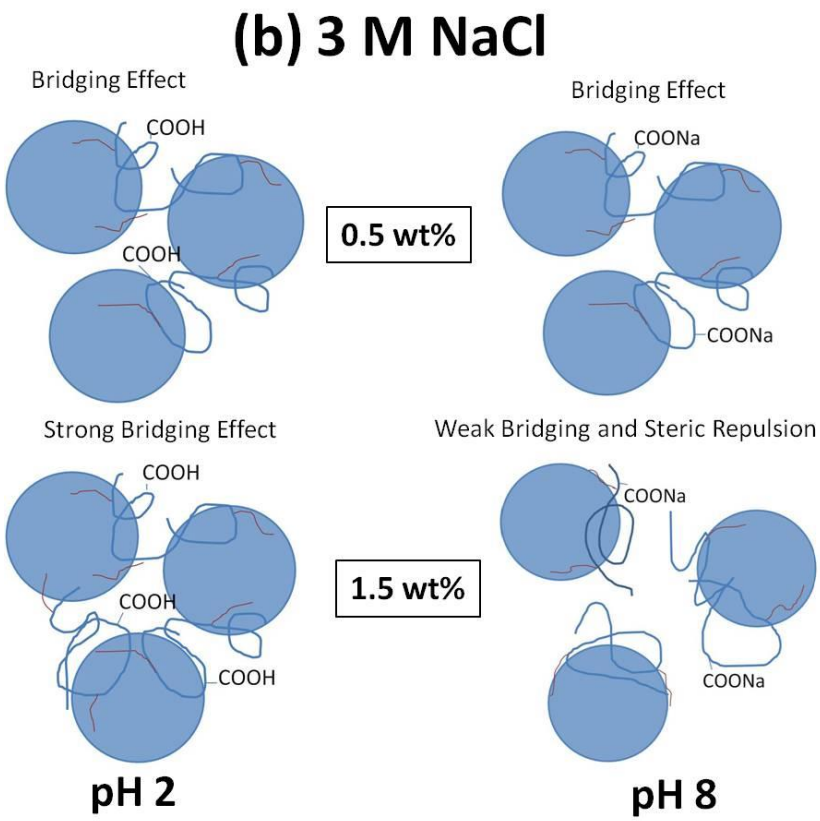


Figure 10. Schematics of the interaction mechanism between PAA/PEO mediated silica particles in 1 mM NaCl (a) and 3 M NaCl (b) solutions at pH 2 (left panels) and pH 8 (right panels).

4. Conclusions

Aqueous suspensions containing model spherical silica particles mediated with comb-type PAA/PEO copolymers under various pH conditions and salt concentrations have been systematically characterized by zeta potential, QCM-D, SFA and rheology measurements. QCM-D results show that the high salinity condition (3 M NaCl) at pH 8 significantly enhances the polymer adsorption on silica as compared to the low salinity case, due to the suppression of electrical double layer. This phenomenon is aligned with a lower zeta potential of silica particles

in the presence of polymers under high salinity condition than that in 1 mM NaCl solution. SFA results reveal that in low salinity solution bridging attraction dominates at low polymer concentration while steric repulsion becomes more significantly at high polymer concentration, which agrees with the QCM-D adsorption results. In 3 M NaCl solution, polymer induced bridging effect is observed under both low and high polymer concentrations based on SFA measurements. The rheology study shows an opposite trend of pH dependent yield stress for silica suspension in 3 M NaCl solution as compared to that in 1 mM NaCl solutions due to the presence and competition of the DLVO (e.g., van der Waals, electrical double layer interactions) and non-DLVO interactions (e.g., polymer bridging due to hydrogen bonding and interpenetration of polymer chains, steric interaction, and ion-correlation interactions). The shear yield stress of silica suspension increases at PAA/PEO concentration from 0 to 0.5 wt% due to bridging effect while it decreases at PAA/PEO concentration from 0.5 to 2 wt% mainly due to the enhanced steric repulsion. These rheological results are well aligned with the QCM-D and SFA force measurements. This work has provided useful results on how solution salinity affects the surface properties and rheology behaviors of colloidal suspensions in the presence of polymer additives, and the methodologies can be readily extended to many other polymer-mediated colloidal systems.

Acknowledgments

The authors gratefully acknowledge the financial support from the Natural Sciences and Engineering Research Council of Canada (NSERC) and the Canada Research Chairs Program (H. Zeng).

References

1. A. O. Emmanuel, F. A. Oladipo, O. E. Ogunsanmi, *J. Sustainable Dev*., 2012, **5**, 74-82.

2. S. Wang, L. Zhang, B. Yan, H. Xu, Q. Liu, H. Zeng, *J. Phys. Chem. C*, 2015, **119**, 7327-7339.

3. D.V. Boger, *Annu. Rev. Chem. Biom. Eng*., 2013, **4**, 239-257.

4. Z. Gao, L. Xie, X. Y. Hu, W. Sun, Cui, H. Zeng, *Langmuir*, 2018, **34**, 2511-2521.

5. M. Amani, K. J. Hassiba, SPE Kuwait International Petroleum Conference and Exhibition, Kuwait, December 10-12, 2012.

6. C. W. Angle, In *Encyclopedic Handbook of Emulsion Technology*, ed. J. Sjoblom, Marcel Dekker: New York, 2001; pp 541-594.

7. M. Neuville, G. Bossis, J. Persello, O. Volkova, P. Boustingorry, M. Mosquet, *J. Rheol*., 2012, **56**, 435.

8. Q. Liu, M. P. Shake, D. R. Blackburn, S. Hinshaw, US Pat. Appl. 2006/0278129 A1, 2006.

9. Q. Ran, P. Somasundaran, C. Miao, J. Liu, S. Wu, J. Shen, *J. Coll. Inter. Sci*., 2009, **336**, 624-633.

10. G.V. Franks, *J. Coll. Inter. Sci*., 2002, **249**, 44-51.

11. R. J. Flatt, I. Schober, E. Raphael, C. Plassard, E. Lesniewska, *Langmuir*, 2008, **25**, 845-855.

12. A. A. Polotsky, T. M. Birshtein, A. A. Mercurieva, F. A. M. Leermakers, O. V. Borisov, *Soft Matt*., 2017, **13**, 9147-9161.

13. E. Laarz, A. Kauppi, K. M. Andersson, A. M. Kjeldsen, L. Bergstrom, *J. Am. Ceram. Soc.* 2006, **89**, 1847-1852.

14. L. Zhang, Q.Y. Lu, Z. Xu, Q.X. Liu, H. Zeng, *J. Colloid Inter. Sci*. 2012, **378**, 222–231.

15. A. Kauppi, K. M. Andersson, L. Bergstrom, *Cemen. Concr. Res*., 2005, **35**, 133-140.

16. C. P. Whitby, P. J. Scales, F. Grieser, T. W. Healy, G. Kirby, J. A. Lewis, C. F. Zukoski, *J. Colloid Inter. Sci*., 2003, **262**, 274-281.

17. H. Hommer, *J. Euro. Ceram. Soc*., 2009, **29**, 1847.

18. J.F. Morris, *Rheol. Acta*. 2009, **48**, 909-923.

19. D. Yang, A. N. Hrymak, *Appl. Rheol*. 2013, **23**, 23622.

20. I. M. Krieger, T. J. Dougherty, *J .Rheol*., 1959, **3**, 137-152.

21. N. J. Wagner, J. Mewis, *Colloidal Suspension Rheology*, Cambridge, 2011.

22. E. Bobicki, Q. Liu, Z. Xu, *Miner. Eng*., 2014, **61**, 97-104.

23. D. Yang, L. Xie, E. Bobicki, Z. Xu, Q. Liu, H. Zeng, *Langmuir*, 2014, **30**, 10809-10817.

24. Y. Wang, L. Wang, M. A. Hampton, A. V. Nguyen, *J. Phys. Chem. C*. 2013, **117**, 2113-2120.

25. S. Savarmand, P. J. Carreau, F. Bertrand, D. J. Vidal, M. Moan, *J. Rheol*., 2003, **47**, 1133.

26. G. V. Franks, S. B. Johnson, P. J. Scales, D. V. Boger, T. W. Healy, *Langmuir*, 1999, **15**, 4411-4420.

27. G. Sauerbrey, *Z. Phys*., 1959, **155**, 206.

28. I. Reviakine, D. Johannsmann, R. P. Richter, *Anal. Chem*. 2011, **83**, 8838-8848.

29. J. Israelachvili, Y. Min, M. Akbulut, A. Alig, G. Carver, W. Greene, K. Kristiansen, E. Meyer, N. Pesika, K. Rosenberg., H. Zeng, *Rept. Prog. Phys*., 2010, **73**, 036601.

30. C. Lim, J. Huang, S. Kim, H. Lee, H. Zeng, D. S. Hwang, *Angew. Chem. Int. Ed*., 2016, **55**, 3343-3346.

31. D. S. Hwang, M. J. Harrington, Q. Lu, A. Masic, H. Zeng, J. H. Waite, *J. Mater. Chem*., 2012, **22**, 15530-15533.

32. H. Zeng, Y. Tian, T. H. Anderson, M. Tirrell, J. N. Israelachvili, *Langmuir*, 2008, **24**, 1173-1182.

33. Y. Tian, J. Wan, N. Pesika, M. Zhou, *Scientific Rept*., 2013, **3**, 1382.

34. K. Kristiansen, P. McGuiggan, G. Carver, C. Meinhart, J. Israelachvili, *Langmuir*, 2008, **24**, 1541-1549.

35. X. Liu, K. Feilberg, W. Yan, E. Thormann, *Langmuir*, 2017, **33**, 4426-4434.

36. J. Mewis, N.J. Wagner, *Colloidal Suspension Rheology*; Cambridge University Press: UK, 2012.

37. L. Alagha, S. Wang, L. Yan, Z. Xu, J. Masliyah, *Langmuir*, 2013, **29**, 3989.

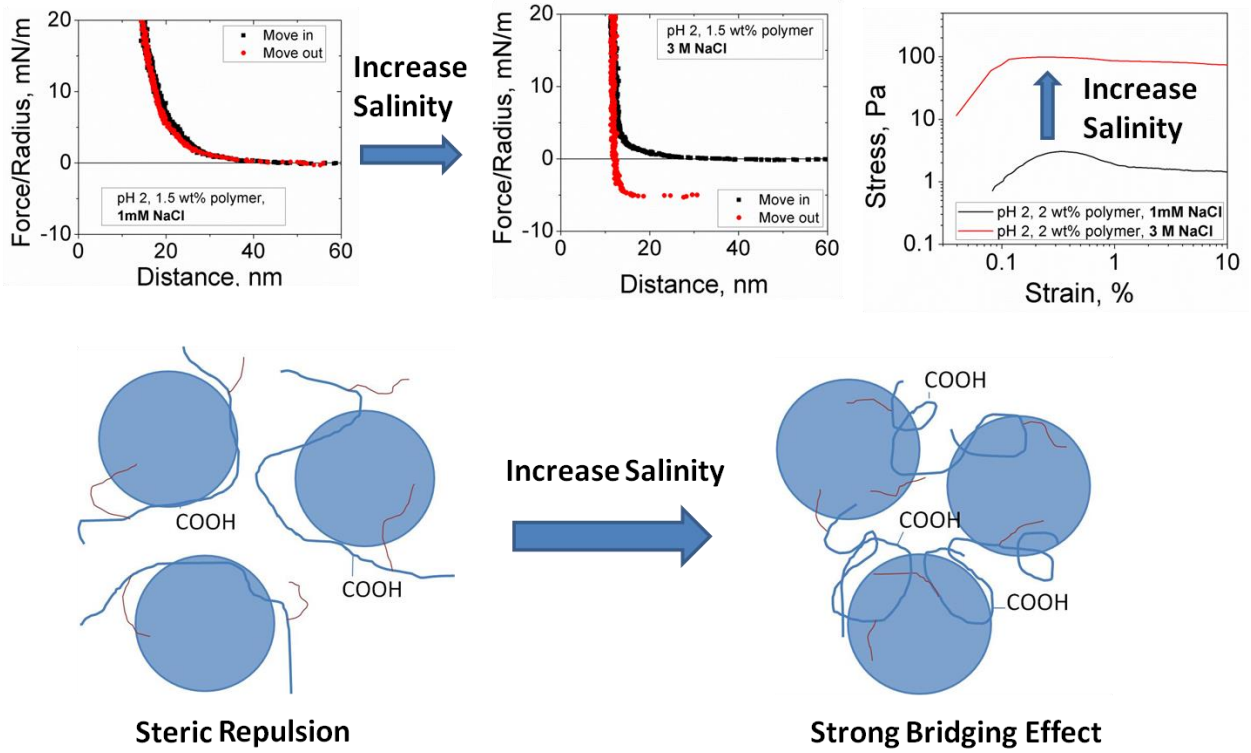
38. J.L. Rosenholtz, D.T. Smith, *American Mineralogist* 1936, **21**, 115-120.

39. L. Bergstrom, *Adv. Colloid Inter. Sci.* 1997, **70**, 125-169.

40. T. Baimpos, B. R. Shrestha, S. Raman, M. Valtiner, *Langmuir*, 2014, **30**, 4322-4332.

41. Q. Tan, G. Zhao, Y. Qiu, Y. Kan, Z. Ni, Y. Chen, *Langmuir*, 2014, **30**, 10845-10854.

TOC Figure


Force/Radius, mN/m
Distance, nm
Move in
Move out
pH 2, 1.5 wt% polymer,
1mM NaCl
Increase
Salinity
pH 2, 1.5 wt% polymer
3 M NaCl
Stress, Pa
Strain, %
pH 2, 2 wt% polymer, 1mM NaCl
pH 2, 2 wt% polymer, 3 M NaCl
COOH
Increase Salinity
Steric Repulsion
Strong Bridging Effect